

# Solvation Dynamics of a Protein in the Pre Molten Globule State

Soma Samaddar,<sup>†,‡</sup> Amit Kumar Mandal,<sup>†</sup> Sudip Kumar Mondal,<sup>‡</sup> Kalyanasis Sahu,<sup>‡</sup>  
Kankan Bhattacharyya,<sup>\*,‡</sup> and Siddhartha Roy<sup>\*,†,§</sup>

Department of Biophysics, Bose Institute, P 1/12 CIT, Scheme VIIM, Kolkata 700 054, Physical Chemistry  
Department, Indian Association for the Cultivation of Science, Jadavpur, Kolkata 700 032, and Indian Institute  
of Chemical Biology, 4 Raja S.C. Mullick Road, Kolkata 700 032, India

Received: July 2, 2006; In Final Form: August 19, 2006

The nature of solvent molecules around proteins in native and different non-native states is crucial for understanding the protein folding problem. We have characterized two compact denatured states of glutamyl-tRNA synthetase (GlnRS) under equilibrium conditions in the presence of a naturally occurring osmolyte, L-glutamate. The solvation dynamics of the compact denatured states and the fully unfolded state has been studied using a covalently attached probe, acrylodan, near the active site. The solvation dynamics progressively becomes faster as the protein goes from the native to the molten globule to the pre molten globule to the fully unfolded state. Anisotropy decay measurements suggest that the pre-molten-globule intermediate is more flexible than the molten globule although the secondary structure is largely similar. Dynamic light scattering studies reveal that both the compact denatured states are aggregated under the measurement conditions. The implications of solvation dynamics in aggregated compact denatured states have been discussed.

## 1. Introduction

Compact denatured states of proteins are of great interest in many fields.<sup>1,2</sup> They are intermediates of folding pathways, and their characterization has been instrumental in understanding the process of protein folding. Recent work indicates that the compact denatured states may also be involved in protein aggregation and fibril formation in vivo, which may lead to many degenerative diseases.<sup>3–5</sup> Among the compact denatured states, the molten globule state is the most well-characterized.<sup>6</sup> Another compact denatured state, called pre molten globule, has been proposed—having less order than the molten globule.<sup>7,8</sup> The pre molten globule state has no rigid tertiary structure. It is characterized by a considerable degree of secondary structure formation, although less pronounced than that of the native or perhaps molten globule state. The protein molecule in the pre molten globule state is somewhat less compact than in the molten globule or native states, but it is still far more compact than the unfolded state. The protein molecule in the pre molten globule state can effectively interact with the hydrophobic fluorescent probe ANS (1-anilino-8-naphthalenesulfonate), although the interaction is weaker than in the molten globule state.<sup>7,9</sup> It has been suggested that pre molten globules may be more important from the perspective of aggregation and fibril formation.<sup>3</sup> The balance of forces that lead to formation of these different classes of compact denatured states is not well understood. Solvation plays a crucial role in determining the relative stability of the states. Hence, solvation dynamics may shed light on the underlying causes of compact denatured state formation under different conditions.

Glutamyl-tRNA synthetase from *Escherichia coli* is a large monomeric protein (MW 64500) having four domains.<sup>10</sup> GlnRS may be a good system to address many of the questions related to unfolding–folding behavior of large proteins. Previously, urea-induced equilibrium denaturation behavior of GlnRS clearly demonstrated the existence of a molten globule in low urea concentrations, but no other significantly populated intermediate could be detected.<sup>11</sup> In this paper, we show that, in the presence of 0.25 M L-glutamate, a naturally occurring osmolyte in *E. coli*, a pre molten globule state is also populated under similar urea concentrations.<sup>12</sup> We also report the solvation dynamics and flexibility of these key protein folding intermediates and discuss their implications for folding and aggregation.

## 2. Experimental Methods

**2.1. Materials.** Ultrapure urea was purchased from Sigma Chemical Co. (St. Louis, MO). ANS and acrylodan were obtained from Molecular Probes. All other chemicals were of analytical grade.

**2.2. Enzyme Purification.** Glutamyl-tRNA synthetase was purified according to Bhattacharyya et al.,<sup>13</sup> and the concentration was determined using  $E^{1\%}_{280} = 10.2$ .<sup>14</sup>

**2.3. Enzyme Labeling.** Acrylodan labeling and characterization have been carried out as described before.<sup>15</sup>

**2.4. Equilibrium Denaturation Studies.** Urea denaturation experiments were performed by diluting the stock enzyme solution with different volumes of buffer (0.1 M Tris–HCl, pH 7.5, containing 0.25 M L-Glu) and a standard urea solution in the same buffer in such a way as to attain the desired final enzyme and urea concentrations. The solutions were then incubated overnight to attain complete equilibrium. The details have been described elsewhere.<sup>11</sup>

**2.5. Spectroscopic Methods.** Fluorescence measurements were carried out in a Hitachi F3010 spectrofluorometer. The excitation and emission band-passes were 3 nm each. For measurement of ANS fluorescence, 30  $\mu$ M ANS was mixed

\* To whom correspondence should be addressed. (S.R.) Phone: 91-33-2473-5368. Fax: 91-33-2473-5197. E-mail: sidroy\_kolkata@rediffmail.com or director@iicb.res.in. (K.B.) Phone: 91-33-2473-3542. Fax: (91)-33-2473-2805. E-mail: pckb@mahendra.iacs.res.in.

<sup>†</sup> Bose Institute.

<sup>‡</sup> Indian Association for the Cultivation of Science.

<sup>§</sup> Indian Institute of Chemical Biology.

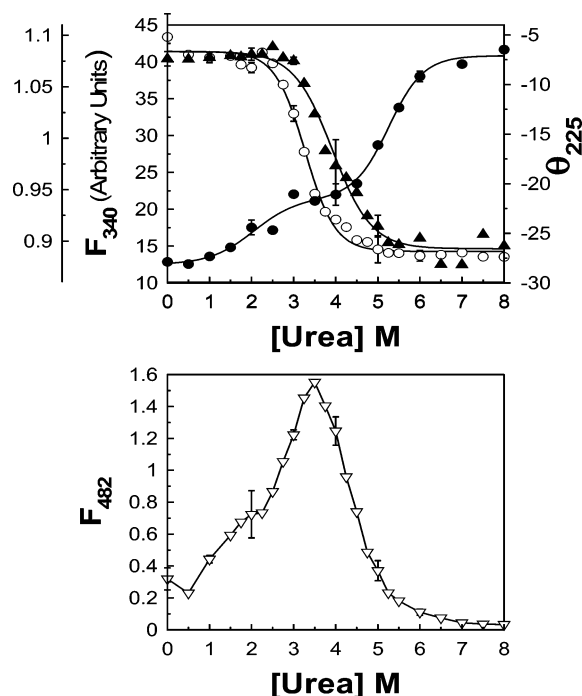


**Figure 1.** Change of spectroscopic signals of glutaminyl-tRNA synthetase (GlnRS) as a function of urea concentration under equilibrium conditions in the presence of 0.25 M potassium L-glutamate: (A, top) (open circles) fluorescence intensity at 340 nm when excited at 295 nm, (solid triangles)  $F_{340}/F_{350}$  of tryptophan fluorescence when excited at 295 nm, (solid circles) CD signal at 225 nm; (B, bottom) ANS fluorescence at 482 nm when excited at 420 nm. Protein concentrations were 2 and 7.5  $\mu\text{M}$  for the fluorescence and CD experiments, respectively. The solution conditions were 0.1 M Tris-HCl buffer, pH 7.5, containing 0.25 M L-Glu and indicated concentrations of urea. The temperature was 25  $^{\circ}\text{C}$ . Error bars indicate the standard error obtained from three independent measurements.

with the protein at a given urea concentration, and the sample fluorescence was measured. A 30  $\mu\text{M}$  concentration was chosen because binding isotherms indicated that beyond this concentration some degree of saturation may occur. The excitation wavelength was 420 nm, and the emission wavelength was 482 nm. The emission wavelength was fixed at 482 nm because this is around the emission maximum of ANS bound to molten globule states of several proteins. Far-UV CD spectra were measured in a Jasco J-600 spectropolarimeter using a 1 mm path length cuvette. Five spectra were signal-averaged for improvement of the signal-to-noise ratio. GlnRS concentrations were 7.5  $\mu\text{M}$  for CD experiments and 2  $\mu\text{M}$  for fluorescence.

**2.6. Solvation Dynamics.** For time-resolved measurements, the samples were excited at 405 nm using a picosecond diode laser (IBH Nanoled-07) of pulse width 70 ps at a repetition rate of 800 kHz. The fluorescence was dispersed using a monochromator (Applied Photophysics,  $f = 3.4$ ). To obtain time-resolved emission spectra, 10 decays were recorded at intervals of 10–15 nm using a 5 nm slit width. The exciting laser beam (at 405 nm) scattered by the sol-gel sample was blocked using a Melles Griot filter. The fluorescence decays were collected at a magic angle polarization using an analyzer and a Hamamatsu MCP photomultiplier (2809U). The time-correlated single photon counting (TCSPC) setup consists of an Ortec 935 QUAD CFD and a Tencel TC 863 TAC. The data are collected with a PCA3 card (Oxford) as a multichannel analyzer. The typical fwhm of the system response is about 100 ps. The fluorescence decays were deconvoluted using global lifetime analysis software (Photon Technology International) in which both the

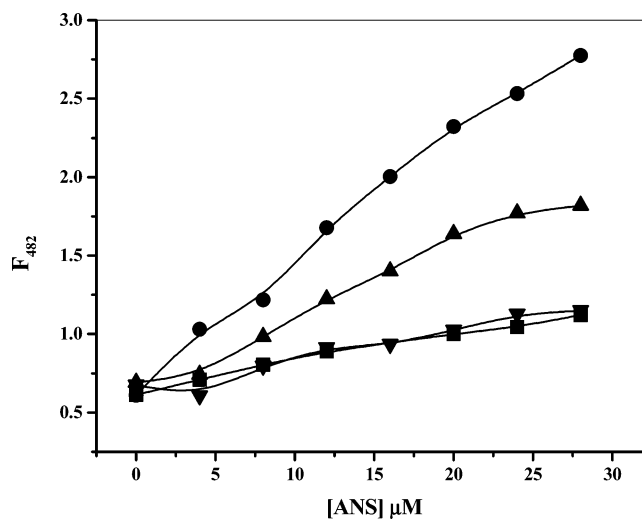


**Figure 2.** ANS fluorescence at 482 nm when excited at 420 nm at different ANS concentrations for the native (solid squares, no urea), molten globule (solid circles, 3.5 M urea), pre molten globule (solid triangles, 4.5 M urea), and unfolded (solid inverted triangles, 7.5 M urea) states. The solution conditions were 0.1 M Tris-HCl buffer, pH 7.5, containing 0.25 M L-Glu and indicated concentrations of urea. The temperature was 25  $^{\circ}\text{C}$ .

lifetimes and amplitudes of the individual decays were allowed to vary freely. The solvation dynamics of probe acrylodan covalently bound to GlnRS was determined for the molten globule (3.5 M urea), pre molten globule (4.5 M urea), and unfolded (7.5 M urea) states in 0.1 M Tris-HCl, pH 7.5, containing 0.25 M L-Glu.

**2.7. Fluorescence Anisotropy Decay.** The decay of time-resolved fluorescence anisotropy provides direct information on the orientational motion of a fluorophore in an organized assembly. The time-dependent fluorescence anisotropy,  $r(t)$ , is given by

$$r(t) = \frac{I_{\parallel}(t) - GI_{\perp}(t)}{I_{\parallel}(t) + 2GI_{\perp}(t)}$$

where  $G$  is a correction factor for instrumental anisotropy. To study fluorescence anisotropy decay, the analyzer was rotated at regular intervals to obtain perpendicular ( $I_{\perp}$ ) and parallel ( $I_{\parallel}$ ) components ( $\lambda_{\text{em}} = 450 \text{ nm}$ ). The  $G$  value of the setup was determined using a probe whose rotational relaxation is very fast, e.g., Nile red in methanol, and the  $G$  value was found to be 1. Anisotropy decay experiments of the probe acrylodan covalently bound to GlnRS were done for the native, molten globule (3.5 M urea), pre molten globule (4.5 M urea), and unfolded (7.5 M urea) states in 0.1 M Tris-HCl, pH 7.5, containing 0.25 M L-Glu.

**2.8. Dynamic Light Scattering.** Dynamic light scattering (DLS) experiments were performed using a DLS 700 instrument (Otsuka Electronics, Japan). For DLS experiments, the protein concentration was kept at 1–7.5  $\mu\text{M}$  and the L-glutamate concentration was kept at 250 mM. In the experiment the sample was illuminated with a 638.8 helium-neon solid-state laser, and the intensity of light scattered at an angle of  $90^{\circ}$  was measured. An autocorrelation function was used to determine the translational diffusion coefficient ( $D_T$ ) of the sample particles in solution by measuring the fluctuations in the intensity of the scattered light. The hydrodynamic radius ( $R_H$ ) of the sample particles was derived from  $D_T$  using the Stoke-Einstein equation

$$D_T = K_b T / 6\pi\eta R_H$$

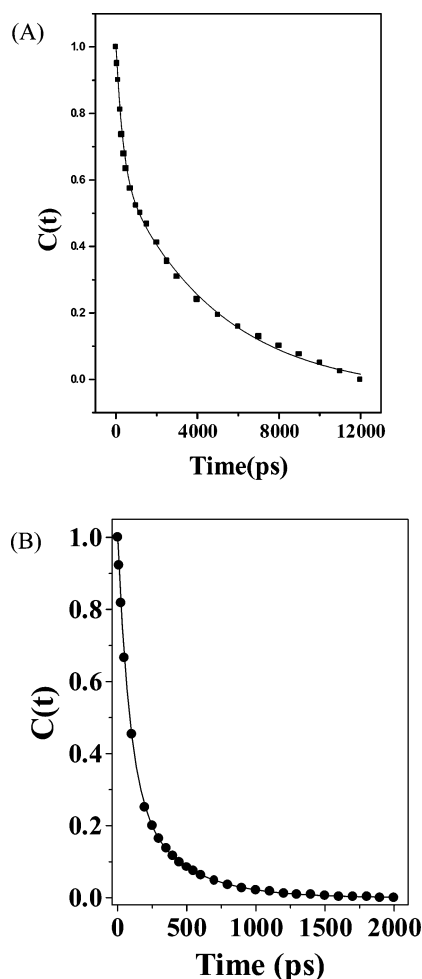


**Figure 3.** Decay of the response function  $C(t)$  of acrylodan covalently bound to GlnRS in the presence of 0.25 M L-Glu in Tris-HCl buffer, pH 7.5, containing (A) 3.5 M urea and (B) 7.5 M urea. The points denote the actual values of  $C(t)$ , and the solid line denotes the best fit to a biexponential decay.

where  $K_b$  is the Boltzmann constant,  $T$  is the absolute temperature (K), and  $\eta$  is the solvent viscosity.

### 3. Results

**3.1. Equilibrium Denaturation.** The equilibrium unfolding study of GlnRS was done in 0.1 M Tris, pH 7.5, in the presence of 0.25 M L-glutamate. In a previous study we detected an intermediate of the molten globule class by equilibrium urea denaturation.<sup>16</sup> Figure 1 shows the plot of the fluorescence intensity, far-UV circular dichroism, ratio of the fluorescence intensities at 340 and 350 nm, and ANS fluorescence in the presence of 0.25 M L-glutamate as a function of urea. There are at least three distinct transitions, implying the presence of at least two intermediates other than the native and unfolded states (we designate them  $I_1$  and  $I_2$ ), with  $I_1$  occurring at lower urea concentrations. The first transition is characterized by a large fluorescence intensity decrease but an insignificant emission maximum shift and is centered around 3 M urea (N to  $I_1$ ). The shift of the emission maximum of tryptophan fluorescence occurs at higher urea concentrations than the N to  $I_1$  transition and is centered around 4 M urea ( $I_1$  to  $I_2$ ). The loss of the far-UV circular dichroism signal ( $\theta_{225}$ ) occurs at even higher urea concentrations and is centered around 5.25 M urea ( $I_2$  to D). In general, ANS and bis-ANS bind to the molten globule class with higher fluorescence yields.<sup>17,18</sup> Here, an ANS fluorescence

increase occurs largely below 3 M urea, peaking around 3.5 M urea, followed by a rapid decline. The declining edge is distinct from the transition represented by loss of fluorescence intensity (N to  $I_1$ ) but coinciding with the decrease of  $F_{340}/F_{350}$  and is centered around 4 M urea ( $I_1$  to  $I_2$ ). As was shown before<sup>16</sup> the first transition, characterized by the loss of fluorescence intensity, represents the previously characterized molten globule state.

The shift of the tryptophan emission maximum to the red suggested that the internal hydrophobic residues have become significantly solvent exposed in the  $I_2$  state. However, the far-UV CD spectrum is largely preserved in this state, indicating that the secondary structures are largely preserved. We have also determined the relative binding ability of ANS to different states.<sup>9</sup> Figure 2 shows the ANS binding isotherm of the native, unfolded, and two intermediate states. It is clear that the native and the denatured states bind ANS the weakest, while the molten globule state ( $I_1$ ) binds ANS the best.  $I_2$  falls somewhere between, indicating that ANS can still access the internal hydrophobic sites but has either a lesser affinity or a lesser quantum yield in the bound state compared to the molten globule state. Increased solvent exposure of the internal residues in this state may be responsible for both. The picture that emerges is that of  $I_2$  as a collapsed chain, but largely preserving the secondary structures. Thus, we suggest that  $I_2$  is an intermediate of the pre molten globule class. A phase diagram analysis of the transitions agrees with the two intermediates and is shown in a figure in the Supporting Information.<sup>19</sup>

**3.2. Solvation Dynamics.** Water plays a fundamental role in the structure, dynamics, and biological function of a protein. Precise information on the solvent relaxation at a selected site of a protein has been obtained recently, using tryptophan as an intrinsic solvation probe<sup>20</sup> and a site-selectively labeled covalent probe such as acrylodan or dansyl.<sup>16,21</sup> According to these studies, the dynamics of the water molecules in the hydration shell of a protein displays a slower component compared to that of the bulk water. Recent studies demonstrate that active sites and other internal sites may dramatically slow the solvent relaxation even compared to that of the protein surface waters.<sup>21</sup> This dramatically slower relaxation is directly correlated with the structure and dynamics of the protein region and may be used as a probe of the structure and dynamics. Recent studies indicate that, even in the molten globule state, the water molecules exhibit a considerably long relaxation dynamics, indicating preservation of the nativelike protein structure and dynamics.<sup>22–24</sup>

It was well established in a previous work that GlnRS forms the molten globule in the presence of 3.5 M urea and 0.25 M L-Glu as an osmolyte.<sup>12</sup> The solvation dynamics in the molten globule state of GlnRS was studied using a covalent probe, acrylodan. In 100 mM Tris-HCl buffer, pH 7.5, containing 3.5 M urea and 0.25 M L-Glu, emission decays of the probe covalently bound to GlnRS show marked wavelength dependence. At the blue end (430 nm), the fluorescence decay is biexponential with components of 750 ps (45%) and 3550 ps (55%). At the red end (550 nm) the decay is also biexponential with time constants of 450 and 4150 ps and is preceded by a distinct rise. Following the procedure given by Maroncelli and Fleming,<sup>25</sup> the time-resolved emission spectrum (TRES) was constructed using the parameters of the best fit to the fluorescence decays and the steady-state emission spectrum. The TRES clearly shows a time-dependent Stokes shift of the emission spectrum of acrylodan bound to the GlnRS (data not shown). The solvation dynamics is described by the decay of the solvent

**TABLE 1: Decay Parameters of  $C(t)$  in Different Systems<sup>a</sup>**

system	Stokes shift (cm <sup>-1</sup> )	$a_1$	$\tau_1$ (ps)	$a_2$	$\tau_2$ (ps)	$\langle\tau_s\rangle$ (ps)
GlnRS + 3.5 M urea + 0.25 M L-Glu	810	0.35	320	0.65	4900	3300
GlnRS + 4.5 M urea + 0.25 M L-Glu	1470	0.45	230	0.55	4370	2500
GlnRS + 7.5 M urea + 0.25 M L-Glu	1180	0.70	80	0.30	380	170

<sup>a</sup> Decay parameters of  $C(t)$  in different systems for acrylodan covalently bound to GlnRS in the molten globule (3.5 M urea), pre molten globule (4.5 M urea), and unfolded (7.5 M urea) states in 0.1 M Tris-HCl, pH 7.5, containing 0.25 M L-Glu.

correlation function  $C(t)$

$$C(t) = \frac{\nu(t) - \nu(\infty)}{\nu(0) - \nu(\infty)}$$

where  $\nu(0)$ ,  $\nu(t)$ , and  $\nu(\infty)$  are the peak frequencies at time 0,  $t$ , and  $\infty$ , respectively. The decay of  $C(t)$  is shown in Figure 3; it is readily seen that in the case of  $I_1$  the decay of  $C(t)$  is biexponential, with a fast component of 320 ps (35%) and a slow component of 4900 ps (65%). The average solvation time ( $\langle\tau_s\rangle = \sum a_i \tau_i$ ) is found to be 3300 ps. The total Stokes shift of acrylodan bound to the native GlnRS is found to be 810 cm<sup>-1</sup>. All the data are summarized in Table 1. It is interesting to note that the average solvation time of GlnRS under identical conditions but without L-glutamate is 2200 ps and the Stokes shift is 1107 cm<sup>-1</sup> (data not shown in the table). Clearly, L-glutamate increases solvent relaxation around the probe, suggesting a significant effect on protein solvation. Many theories of osmolyte function hypothesize on the effect of the osmolyte on protein solvation, and our observation is consistent with these theories.<sup>26,27</sup>

In 100 mM Tris buffer, pH 7.5, containing 4.5 M urea and 0.25 M L-Glu, the emission decays of the probe covalently bound to GlnRS also show marked wavelength dependence. At the blue end (410 nm) the fluorescence decay is triexponential with three decay components of 100 ps (40%), 1000 ps (30%), and 3400 ps (30%). At 540 nm (red end) the decay of time constants 2300 and 3850 ps is preceded by a distinct rise of 500 ps. So it may be concluded from the wavelength dependency of the fluorescence decays that the solvation dynamics is also slow here but different from that of the 3.5 M case. The decay of  $C(t)$  is found to be biexponential with a short component of 250 ps (45%) and a long component of 4350 ps (55%) with an average solvation time of 2500 ps. The total Stokes shift is observed to be 1470 cm<sup>-1</sup>.

The solvation dynamics of the acrylodan covalently bound to GlnRS in the fully denatured state was studied in 100 mM Tris buffer, pH 7.5, containing 7.5 M urea and 0.25 M L-Glu. Again emission decays of the probe bound to GlnRS show marked wavelength dependence. At the blue end (450 nm) the fluorescence decay is triexponential with three decay components of 100 ps (50%), 950 ps (30%), and 3500 ps (a long component) (20%). At the red end (600 nm) the decay of time constants 1400 and 3300 ps is preceded by a distinct rise with a time constant of 200 ps. The decay of  $C(t)$  is found to be biexponential with a very short component of 80 ps (70%) and another component of 380 ps (30%) with an average solvation time of 170 ps. Evidently, the previous long component vanishes and is replaced by a shorter component. Interestingly, both of these components are significantly longer than those of acrylodan-labeled human serum albumin,<sup>28</sup> indicating that, even in 7.5 M urea, some structure is present although almost all secondary and tertiary structure is absent. This is not inconsistent with newer ideas of more structured unfolded states than previously believed.<sup>29–31</sup> The total Stokes shift is observed to be 1180 cm<sup>-1</sup>. Clearly, there is a progressive change of solvation

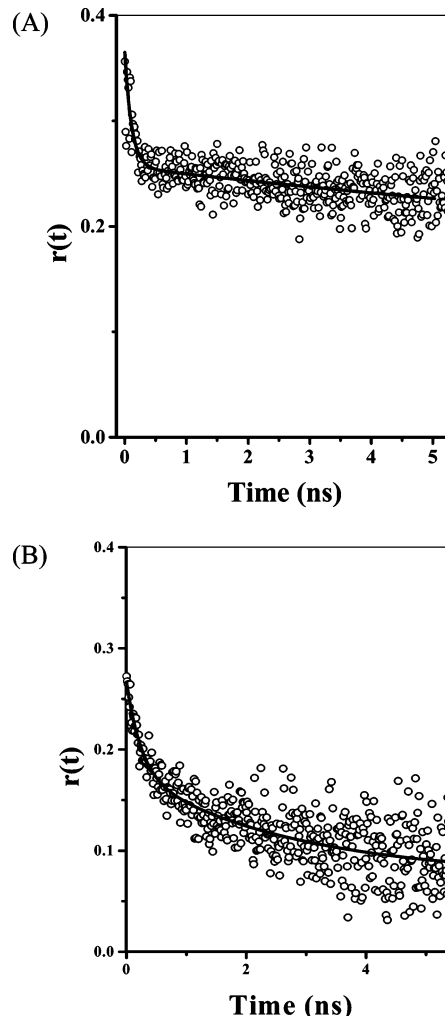


**Figure 4.** Decay of the fluorescence anisotropy of acrylodan covalently bound to GlnRS in 0.1 M Tris-HCl, pH 7.5, containing 0.25 M L-Glu and (A) no urea and (B) 7.5 M urea. The points denote actual values of  $r(t)$ , and the solid lines denote the best fit to a biexponential decay.

dynamics going from the native to the unfolded state. However, the compact denatured states resemble the native state more than the unfolded state.

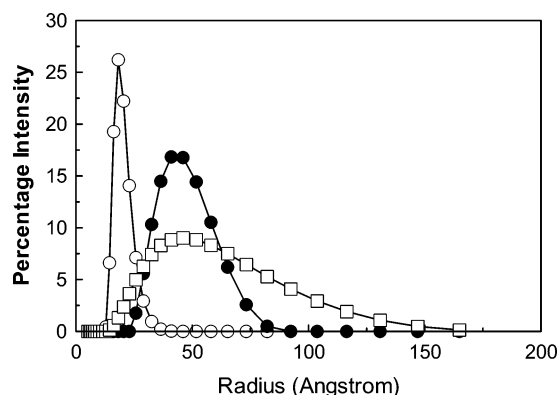
**3.3. Fluorescence Anisotropy Decay.** Fluorescence anisotropy decay of a covalently labeled probe can be a powerful tool for analyzing segmental and global motions of a protein. This can yield useful information complementary to the solvation dynamics. The fluorescence anisotropy decay of acrylodan covalently bound to native GlnRS is shown in Figure 4, and the decay analysis is summarized in Table 2. The anisotropy decay of acrylodan covalently bound to native GlnRS was found to be biexponential with components of 100 ps and 16.7 ns. In the molten globule state ( $I_1$ ), the anisotropy decay consists of one short component, 220 ps, and one long component, 15 ps. Similarly, acrylodan bound to GlnRS in the presence of 4.5 M urea and 0.25 M L-Glu shows two components of 150 ps and 7



TABLE 2: Anisotropy Decay Parameters of Acrylodan Covalently Bound to GlnRS<sup>a</sup>

system	$a_1$	$\tau_1$ (ps)	$a_2$	$\tau_2$ (ns)	$r_0$	$r_a$
native GlnRS	0.5	100	0.5	16.7	0.36	0.23
GlnRS + 3.5 M urea + 0.25 M L-Glu	0.4	220	0.4	15	0.27	0.18
GlnRS + 4.5 M urea + 0.25 M L-Glu	0.6	150	0.4	7	0.32	0.18
GlnRS + 7.5 M urea + 0.25 M L-Glu	0.5	240	0.5	2.27	0.27	0.09

<sup>a</sup> Fluorescence anisotropy decay parameters of acrylodan bound to GlnRS in the native, molten globule (3.5 M urea), pre molten globule (4.5 M urea), and unfolded (7.5 M urea) states in 0.1 M Tris-HCl, pH 7.5, containing 0.25 M L-Glu.



**Figure 5.** Distribution of the particle size measured by DLS. Dynamic light scattering analysis was done at 7.5  $\mu$ M GlnRS in 0.1 M Tris-HCl buffer, pH 7.5, containing 0.25 M L-Glu. The urea concentration was varied from 0 to 4.5 M. The hydrodynamic radius was calculated using the Stokes-Einstein equation. All the data were collected taking an average of 100 scans. Key: (open circles) native, (solid circles) 3.5 M urea, (open squares) 4.5 M urea.

TABLE 3: Distribution of Particle Size Measured by DLS<sup>a</sup>

urea concn (M)	GlnRS concn ( $\mu$ M)	mean % intensity distribution range (size)	peak
0	1	5.7–10.18	7.2
	5	7.18–10.18	8
	7.5	6.4–10.18	8
3.5	1	12–25	16
	2.5	22–40	28
	7.5	31–38	36
4.5	1	12–32	20
	2.5	28–65	42
	7.5	22–82	36

<sup>a</sup> Dynamic light scattering analysis was done using 0–7.5  $\mu$ M GlnRS in 0.1 M Tris buffer, pH 7.5, containing 0.25 M L-Glu. The urea concentration was varied from 0 to 4.5 M. The hydrodynamic radius was calculated using the Stokes-Einstein equation. All the data were collected taking an average of 100 scans.

ns. In the fully unfolded state the decay consists of a 240 ps component and a 2.3 ns component. The fast component is probably due to the local motion of the probe only, which does not significantly change with urea concentration, but the slower component, which is probably due to unresolved segmental motions and the tumbling of the whole protein, becomes faster at higher urea concentrations, indicating a progressive increase of segmental motion. Most importantly,  $I_2$  has significantly increased segmental flexibility compared to  $I_1$ . The fully unfolded state has very rapid segmental motion, as expected.

**3.4. Dynamic Light Scattering.** The hydrodynamic size and the aggregation behavior of the intermediates were studied using DLS. DLS provides a direct measurement of the translational diffusion coefficient ( $D_T$ ). From the value of  $D_T$  the hydrated radius can be calculated using the Stokes-Einstein equation, and also an idea about its molecular weight can be made. Figure 5 and Table 3 summarize the DLS experiments. The measurements were done after the protein denaturation reached equilibrium, and hence, the measurements reflect the signal from an equilibrium ensemble. However, this also indicates the solvation dynamics in the molten and pre molten globule states originates from the aggregated state. It is clear that the native GlnRS hydrated radius does not increase as a function of the protein concentration, and the value is consistent with the expected size of the monomer. In contrast, both  $I_1$  and  $I_2$  show concentration-dependent aggregation behavior. However,  $I_2$  appears to aggregate significantly more than  $I_1$ . The distribution appears to be broader for  $I_2$ , with significant components having a very large hydrated radius.

**4. Discussion**

The solvation shell around a protein molecule plays an important role in determining the stability of different folded states. The solvation dynamics around probes attached to proteins is increasingly being reported. However, only a few studies have been done on the non-native protein states. In a previous paper we showed that equilibrium denaturation of GlnRS produces a compact denatured state at lower urea concentrations.<sup>11</sup> This state showed dramatically reduced tryptophan fluorescence intensity but a natively like emission maximum. ANS binding is also dramatically enhanced in this state. Further increases in urea concentrations led to loss of secondary structure, loss of ANS binding, and a shift of the tryptophan emission spectrum to the red, indicating transition to the unfolded state. In a subsequent paper, we showed that addition of a natural osmolyte, L-glutamate, shifts the urea denaturation profile toward higher urea concentrations without significantly affecting the profile qualitatively.<sup>16</sup> In this paper, a fuller analysis demonstrated that in the presence of L-glutamate another compact denatured state can be detected that exists between the molten globule and the unfolded states. This phenomenon is not restricted to L-glutamate but is qualitatively reproduced in some other osmolytes as well (data not shown). This state ( $I_2$ ) has a secondary structure content that is similar to that of the molten globule ( $I_1$ ) but with reduced ANS binding. Importantly, the tryptophan fluorescence emission maximum is drastically shifted to the red, indicating solvent exposure. Thus, this second compact denatured state has many characteristics of a pre molten globule state proposed by Uversky and co-workers.<sup>7</sup>

#### 4. Discussion

When a fluorescence probe is excited, the surrounding atoms reorganize due to a change in polarity of the excited state. The reorganization may include the solvent molecules around the probe as well as amino acid side chains around the probe. The probe itself may also move, contributing to the observed solvation dynamics. The contribution of these different types of motion to solvation dynamics is difficult to resolve. The role of the motion of the probe itself can be judged by comparing anisotropy decay with solvation dynamics. In this study we have observed that the short component of the solvation dynamics progressively decreases with increasing urea concentrations whereas the short component of the anisotropy decay remains

roughly invariant. This suggests that the short component of the anisotropy decay does not originate from the probe motion but may be a result of motion of the solvent or protein side chains around the probe.

The solvation dynamics of acrylodan attached to C229 indicates that slowly relaxing protein side chains and water molecules around the active site become somewhat faster relaxing compared to those of the native and molten globule states but still much slower relaxing than those of the unfolded state (D). Slower solvation dynamics is well correlated with the constraint imposed on exchange of a bound water molecule with the bulk water—brought in by the rigidity of the three-dimensional structure of the protein as well as other constraints such as additional hydrogen bond formation originating in the three-dimensional structure of the protein.<sup>32,33</sup> Clearly, the pre molten globule has retained much of the folded structure, resulting in slower solvation dynamics, which is more like the native state than the unfolded state. However, significant reduction of relaxation time in the pre molten globule state is a probable indication of enhanced flexibility. Both the molten globule state and the pre molten globule state are however aggregated, with the pre molten globule state having a higher degree of aggregation. Similar behavior was observed with staphylococcal nuclease. Part of the nativelike secondary structure observed in the pre molten globule state may have originated from increased aggregation.<sup>34–36</sup> Anisotropy decay of the probe, although somewhat faster than in the native and the molten globule states, is still much slower than that in the unfolded state. This certainly supports a model of enhanced flexibility in I<sub>2</sub>, in agreement with the conclusions drawn from the solvation dynamics data. The internal tryptophans are largely exposed, but ANS binding is weaker, and the internal hydrophobic patches must be significantly solvent exposed perhaps through enhanced segmental motion. Combining all this information, it appears that the pre molten globule state of GlnRS is a compact state with nativelike secondary structure but having considerable flexibility. The degree of flexibility of the pre molten globule state is significantly higher than that of the molten globule state.

Solvent plays a very important role in the folding process. A gain of solvent entropy in going from the unfolded state to the folded state (due to burial of the hydrophobic surface area) is thought to be a major driving force. However, solvation dynamics results obtained over the past several years also suggest that first-layer hydration water becomes more constrained upon folding, and some loss of solvent entropy on this account is expected in going from the unfolded to the native state.<sup>16,20,24,28,32,33</sup> Although more studies are needed to generalize the conclusions drawn here and other solvation dynamics studies of compact denatured states, tentatively we may conclude that even in the pre molten globule state the solvent surrounding the protein molecules is significantly ordered. Thus, the solvent entropy due to ordering of the first hydration shell is largely sacrificed during the first hydrophobic collapse to a pre molten globule state and hence would not unfavorably affect the transition to an ordered native state at the later stage of the folding process.

## 5. Conclusions

The solvation dynamics of a multidomain protein has been studied in a pre molten globule state, which is devoid of any organized tertiary structure. Interestingly, even in this state the solvation dynamics is slow, compared to that of the unfolded state. This indicates that even collapsed protein chains impose

enough constraints to retard solvation dynamics, even in the absence of any organized tertiary interactions.

**Acknowledgment.** We acknowledge CSIR and DST for research support.

**Supporting Information Available:** A figure showing a phase diagram analysis of the transitions, which displays agreement with the two intermediates. This material is available free of charge via the Internet at <http://pubs.acs.org>.

## References and Notes

- (1) Fink, A. L. *Subcell Biochem.* **1995**, *24*, 27.
- (2) Fink, A. L. *Annu. Rev. Biophys. Biomol. Struct.* **1995**, *24*, 495.
- (3) Uversky, V. N.; Fink, A. L. *Biochim. Biophys. Acta* **2004**, *1698*, 131.
- (4) Dobson, C. M. *Protein Pept. Lett.* **2006**, *13*, 219.
- (5) Uversky, V. N. *Cell. Mol. Life Sci.* **2003**, *60*, 1852.
- (6) Ptitsyn, O. B. *Adv. Protein Chem.* **1995**, *47*, 83.
- (7) Uversky, V. N.; Ptitsyn, O. B. *J. Mol. Biol.* **1996**, *255*, 215.
- (8) Chaffotte, A. F.; Guijarro, J. I.; Guillou, Y.; Delepierre, M.; Goldberg, M. E. *J. Protein Chem.* **1997**, *16*, 433.
- (9) Semisotnov, G. V.; Rodionova, N. A.; Razgulyaev, O. I.; Uversky, V. N.; Gripas, A. F.; Gilmanshin, R. I. *Biopolymers* **1991**, *31*, 119.
- (10) Rould, M. A.; Perona, J. J.; Steitz, T. A. *Nature (London)* **1991**, *352*, 213.
- (11) Lew, V. L.; Raftos, J. E.; Sorette, M.; Bookchin, R. M.; Mohandas, N. *Blood* **1995**, *86*, 334.
- (12) Cayley, S.; Lewis, B. A.; Guttman, H. J.; Record, M. T., Jr. *J. Mol. Biol.* **1991**, *222*, 281.
- (13) Bhattacharyya, T.; Bhattacharyya, A.; Roy, S. *Eur. J. Biochem.* **1991**, *200*, 739.
- (14) Hoben, P.; Royal, N.; Cheung, A.; Yamao, F.; Biemann, K.; Soll, D. *J. Biol. Chem.* **1982**, *257*, 11644.
- (15) Bhattacharyya, T.; Roy, S. *Biochemistry* **1993**, *32*, 9268.
- (16) Mandal, D.; Sen, S.; Sukul, D.; Bhattacharyya, K.; Mandal, A. K.; Banerjee, R.; Roy, S. *J. Phys. Chem. B* **2002**, *106*, 10741.
- (17) Jones, B. E.; Jennings, P. A.; Pierre, R. A.; Matthews, C. R. *Biochemistry* **1994**, *33*, 15250.
- (18) Shi, L.; Palleros, D. R.; Fink, A. L. *Biochemistry* **1994**, *33*, 7536.
- (19) Kuznetsova, I. M.; Turoverov, K. K.; Uversky, V. N. *J. Proteome Res.* **2004**, *3*, 485.
- (20) Peon, J.; Pal, S. K.; Zewail, A. H. *Proc. Natl. Acad. Sci. U.S.A.* **2002**, *99*, 10964.
- (21) (a) Guha, S.; Manna, T. K.; Das, K. P.; Bhattacharyya, B. *J. Biol. Chem.* **1998**, *273*, 30077. (b) Guha, S.; Sahu, K.; Roy, D.; Mondal, S. K.; Roy, S.; Bhattacharyya, K. *Biochemistry* **2005**, *44*, 8940.
- (22) Denisov, V. P.; Jonsson, B. H.; Halle, B. *Nat. Struct. Biol.* **1999**, *6*, 253.
- (23) Lindorff-Larsen, K.; Paci, E.; Serrano, L.; Dobson, C. M.; Vendruscolo, M. *Biophys. J.* **2003**, *85*, 1207.
- (24) Sahu, K.; Mondal, S. K.; Ghosh, S.; Roy, D.; Sen, P.; Bhattacharyya, K. *J. Phys. Chem. B* **2006**, *110*, 1056.
- (25) Maroncelli, M.; Fleming, G. R. *J. Chem. Phys.* **1987**, *86*, 6221.
- (26) Zou, Q.; Bennion, B. J.; Daggett, V.; Murphy, K. P. *J. Am. Chem. Soc.* **2002**, *124*, 1192.
- (27) Shimizu, S. *J. Chem. Phys.* **2004**, *120*, 4989.
- (28) Kamal, J. K.; Zhao, L.; Zewail, A. H. *Proc. Natl. Acad. Sci. U.S.A.* **2004**, *101*, 13411.
- (29) Tang, Y.; Rigotti, D. J.; Fairman, R.; Raleigh, D. P. *Biochemistry* **2004**, *43*, 3264.
- (30) Mayor, U.; Grossmann, J. G.; Foster, N. W.; Freund, S. M.; Fersht, A. R. *J. Mol. Biol.* **2003**, *333*, 977.
- (31) Pappu, R. V.; Srinivasan, R.; Rose, G. D. *Proc. Natl. Acad. Sci. U.S.A.* **2000**, *97*, 12565.
- (32) Nandi, N.; Bhattacharyya, K.; Bagchi, B. *Chem. Rev.* **2000**, *100*, 2013.
- (33) Nandi, N.; Bagchi, B. *J. Phys. Chem. B* **1997**, *101*, 10954.
- (34) Uversky, V. N.; Karnoup, A. S.; Segel, D. J.; Seshadri, S.; Doniach, S.; Fink, A. L. *J. Mol. Biol.* **1998**, *278*, 879.
- (35) Uversky, V. N.; Karnoup, A. S.; Khurana, R.; Segel, D. J.; Doniach, S.; Fink, A. L. *Protein Sci.* **1999**, *8*, 161.
- (36) Uversky, V. N.; Segel, D. J.; Doniach, S.; Fink, A. L. *Proc. Natl. Acad. Sci. U.S.A.* **1998**, *95*, 5480.